

In situ ion etching in a scanning electron microscope

R. S. DHARIWAL, R. K. FITCH

Department of Physics, University of Aston in Birmingham, UK

A facility for ion etching in a scanning electron microscope is described which incorporates a new type of electrostatic ion source and viewing of the specimen is possible within about 30 sec after terminating the ion bombardment. Artefacts produced during etching have been studied and cone formation has been followed during its growth. The instrument has provided useful structural information on metals, alloys and sinters. However, although insulating materials, such as plastics, glass and resins, have been successfully etched, interpretation of the resultant micrographs is more difficult. Ion etching of soft biological tissues, such as the rat duodenum was found to be of considerable interest. The observed structural features arise from the selective intake of the heavy fixation elements by different parts of the tissue. Hard biological materials, such as dental tissues and restorative materials, have also been studied and the prismatic structure of the enamel and the form and distribution of the dentinal tubules have been revealed.

1. Introduction

In the last decade the technique of sputter ion etching has become widely used as exemplified by the various applications discussed in recent articles by Gloersen [1] and Norgate and Hammond [2]. In one application the etching technique is used to reveal the microstructure of materials prior to examination in a scanning electron microscope (SEM). However, in the majority of cases reported in the literature, the ion etching process has been carried out in a separate ion beam system. This requires frequent transfer of the specimen from the ion beam system to the SEM. It is thus difficult to follow the formation of surface structures and has the further disadvantage that the specimen may be damaged during transfer. Only in a few instances has the ion-source been incorporated into the specimen stage of the SEM for *in situ* ion etching. Stewart [3] modified a microscope to include an r.f. ion source but his system was rather complex and involved three independent pumping systems. Hodges *et al.* [4] incorporated an ion gun into a Cambridge Instruments "Stereoscan" to etch mammalian cells but concluded that the tech-

nique was unlikely to be of much value with soft biological tissues. On the other hand Spector *et al.* [5] using an ETEC ion beam etching device in the specimen chamber of an ETEC Autoscan SEM concluded that the artefact production in red blood cells became less prominent as the ion accelerating voltage was increased and useful sub-surface structure could be revealed. Weissmantel *et al.* [6] used an ion gun inside a JEOL SEM with a cinematographic recording attachment to study the structure of PTFE. Shimizu [7] used a field emission scanning electron micrograph to study surface erosion of ion bombarded copper and gold surfaces, but it is not clear from his paper if the ion gun was attached to the microscope.

The actual type of ion source to be used is one of the most important factors to be considered for *in situ* ion etching in a SEM. It is preferable that it is of simple construction, stable in operation and can produce a reasonably collimated but intense ion beam at low pressures without the assistance of a magnetic field. Furthermore it is desirable that it can be used with insulating materials without some additional facility to neutralize the

charge build up that occurs on these type of specimens.

A source which meets most of these requirements is the saddle field ion source which was developed from the idea of McIlraith [8] for an electrostatic charged-particle oscillator. At present two main types of this source have been developed. The earlier version is of cylindrical geometry and was first described by Fitch *et al.* [9] and later in a more practical form by Rushton *et al.* [10]. The spherical form of this source was devised by Franks [11] and the characteristics of the source were published by Franks and Ghander [12]. Both sources operate at low pressures without a magnetic field or thermionic source of electrons and are therefore eminently suitable for incorporating into the specimen stage of the SEM. Furthermore the beam produced by these sources contains a significant proportion of energetic neutrals and can thus be used to etch non-conducting materials.

The main differences between these two sources is that the spherical source produces a more intense and more monoenergetic beam whereas the cylindrical source gives a more divergent beam with a broader energy spectrum. Thus the former is more suitable for high etching rates whereas the latter is to be preferred if it is necessary to etch a larger area of specimen.

The purpose of this paper is to describe a facility for *in situ* ion etching in a SEM in which both of these sources have been used.

2. Description and operating characteristics of the ion etching facility

The scanning electron microscope used in this investigation is the Vacuum Generators "Miniscan". Its maximum resolution is only about 500 Å but it has the advantage that the specimen chamber can be easily adapted to incorporate other facilities such as the ion source. A schematic diagram of the modified form of the specimen chamber is given in Fig. 1. The ion source can be seen mounted onto a flange attached to a 10 cm diameter port and the figure also shows the position of the viewing window, the scintillator photomultiplier assembly and the goniometer stage. The arrangement did not allow complete variation of the angle of the ion beam with respect to the normal at the specimen and was usually kept at 27°. The specimen, if desired, could be rotated during bombardment by means of a small electric motor attached through a

* HT = high tension.

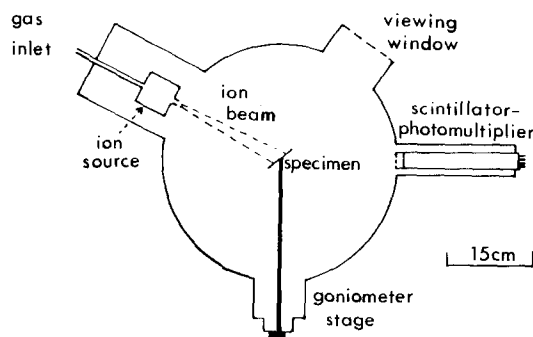


Figure 1 Schematic diagram of the specimen stage of the scanning electron microscope.

gearing mechanism to the main shaft of the goniometer. Argon gas was admitted into the source via a needle valve and during etching the column isolation valve was closed to prevent contamination of the optical column and the pressure in the chamber was maintained at about 2×10^{-5} Torr.

When it is required to view the specimen, the HT* to the ion source is switched off, the column isolation valve is opened and the specimen is turned to the appropriate angle — usually 45° — to the electron beam. With this arrangement it is possible to view the specimen within about 30 sec after terminating the ion bombardment. However with non-conducting materials, if a permanent record of the specimen surface was required with an electron micrograph, it was necessary to remove the specimen from the chamber for coating with a conducting film of gold-palladium alloy.

Throughout the present investigation the operating conditions for the ion sources were kept constant. The cylindrical source was operated at an anode voltage of 8 kV, anode current of 6 mA giving a total beam current of 160 μA and maximum ion beam density in the centre of the beam of about 250 $\mu\text{A cm}^{-2}$ at a chamber pressure of 2×10^{-5} Torr. The corresponding values for the spherical source were 6 kV, 2 mA, 40 μA , 500 $\mu\text{A cm}^{-2}$ and 1.5×10^{-5} Torr. Under the above conditions the maximum etching rate for the cylindrical source was about 5 $\mu\text{m h}^{-1}$ and for the spherical source about 10 $\mu\text{m h}^{-1}$ for an OFHC copper specimen. The maximum temperature achieved by a conducting material during ion bombardment was estimated to be about 75 and 45° C for the cylindrical and spherical sources, respectively. However, with an insulating material these figures increased to about 135 and 80° C, respect-

ively. These were average temperatures of a typical size specimen – 10 mm diameter, 3 mm thick – and were measured using a thermocouple embedded in the specimen which was mounted on the specimen stud and the rate of rise of temperature could be recorded during bombardment. The initial rapid rise is from the heating of the specimen by the ion beam, whereas the much slower rise to the final equilibrium temperature – attained after between 1 and 2 h – is a consequence of the low thermal conductivity of the specimen and/or the thermal inertia of the whole system.

The possibility of contamination of the specimen by material sputtered from the inside of the ion source cathode was investigated using a VG* ESCA instrument. It was anticipated that likely contamination from the cylindrical source would be iron, chromium and nickel and from the spherical source, aluminium. High purity copper foil was ion etched for 6 h but the resulting ESCA analysis did not show any of the above impurities within the limit of detection of about 1%.

3. Artefacts produced during ion bombardment

It is now well known that structural features observed on ion bombardment surfaces may not be characteristic of the material but may be artefacts. However, the distribution of these artefacts across the surface is, in general, quite random and can usually be clearly identified. The most commonly observed artefacts are the cone-like structures which were first observed in the optical microscope by Guntherschulze and Tollmein [13]. Cones have since been observed in the scanning electron microscope by many workers for example, Stewart and Thompson [14] and Wehner

and Hajicek [15]. It is generally accepted that these cones are caused by particles on the surface, or by inclusions in the matrix, which have a lower sputtering yield than the matrix itself. However, other observed structures such as hummocks cannot be explained on this basis and Barber *et al.* [16] have developed a satisfactory theory based on Frank's kinematic theory of crystal dissolution, which predicts the various observed surface topographies of ion bombarded surfaces. In the present work cones have been observed on metals, insulators and biological materials.

Fig. 2a shows a perfectly symmetrical cone produced on a copper surface after etching for 14 h. The height of the cone is about $60\ \mu\text{m}$ and the circumferential ditch at the base of the cone is believed to be caused by the increase of the ion flux due to ion reflection from the sides of the cone [17]; In contrast, other remarkable features were observed on an Araldite surface after etching for 16 h and are shown in Fig. 2b. The micrograph shows clusters of pillar-like cones some of which have whisker-like growths, several times the height of the cone, extending from the tip. Some of these whiskers have already fallen off the cones. In the present work, although a relatively large number of materials have been studied, these effects have only been observed on Araldite. At this stage no satisfactory explanation can be given to explain these effects but it is possible that they may be due to fibrous inclusions in the material similar to that reported by Witcomb [18] in stainless steel.

In one particular investigation the growth of a cone on an Araldite surface was followed during ion etching over a period of 130 h. Micrographs were taken at regular intervals and Fig. 3a, b, c and d show four selected stages of growth of the cone

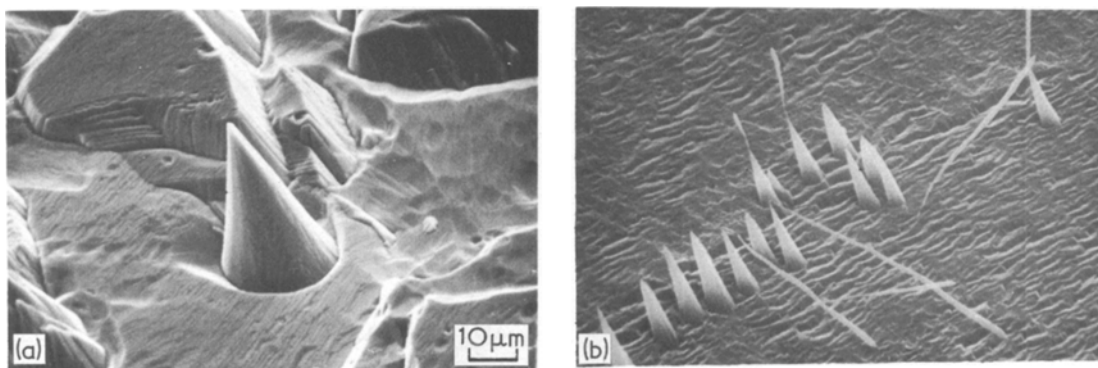


Figure 2 Artefacts produced by ion etching on (a) copper and (b) Araldite.

* VG = Vacuum Generator.

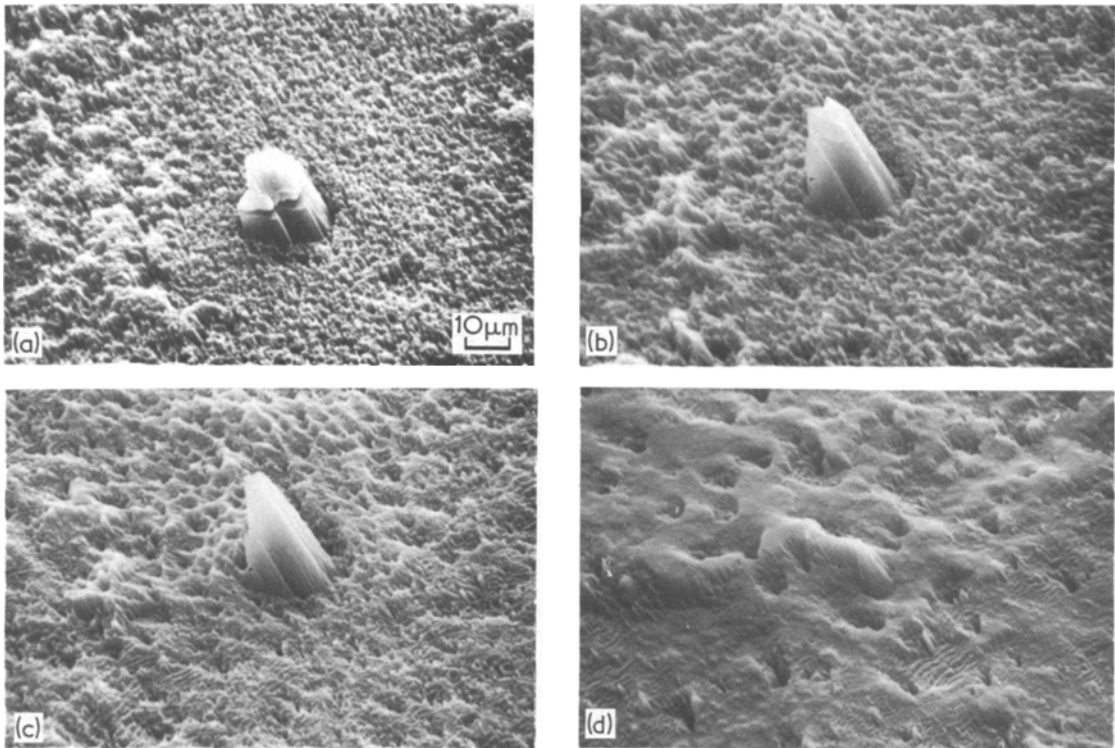


Figure 3 Various stages during the growth of a cone on Araldite.

after 14, 44, 80 and 130 h respectively. It can be seen that while the shielding particle remains, the structure grows to a maximum height of about $50\ \mu\text{m}$. After the true cone-like structure is revealed in Fig. 3c, when the particle has been removed, the cone is gradually eroded away as in Fig. 3d.

All the cone-like artefacts observed during this investigation were produced with the specimen stationary during etching but none were observed when the specimen was continually rotated during etching. This is to be expected from the model of cone formation already discussed and it would

thus appear to be advantageous to rotate the specimen. However, this is frequently offset by the fact that this also results in a loss of the desired structural features of the specimen. Furthermore the presence of a small number of cones can be advantageous as they provide a permanent record on the micrograph of the direction of the incident ion beam.

4. Structural effects arising from ion etching various materials

In order to assess the value of this *in situ* ion etching facility, it has been applied to a wide

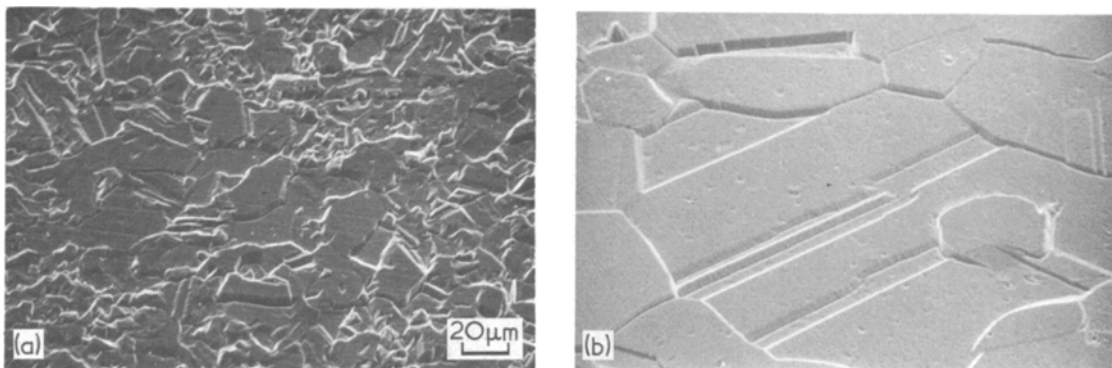


Figure 4 Etched surfaces of copper after annealing at (a) 400°C and (b) 700°C .

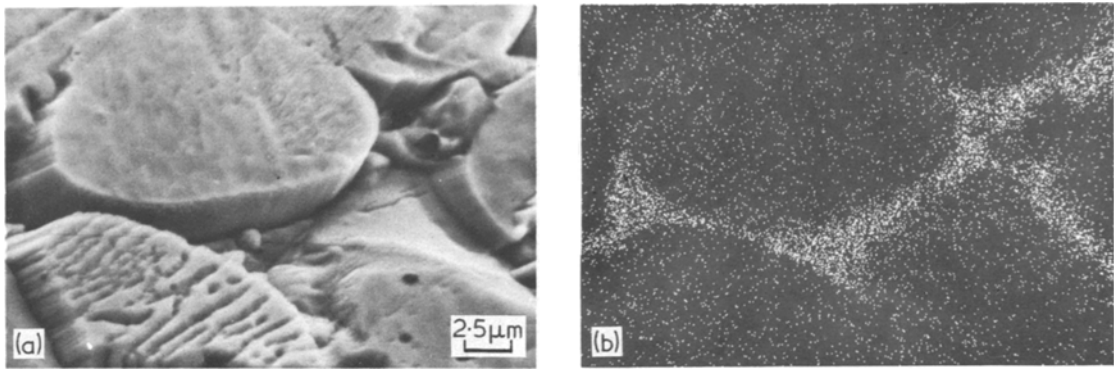


Figure 5 (a) Ion etched surface of a copper-iron sinter. (b) Copper X-ray image of (a) showing the distribution of copper at the grain boundaries (by kind permission of Lucas Group Research, Solihull).

variety of materials taken from actual problems in industrial, research and university laboratories. A selection of these is given in this paper.

Problems are often encountered when studying the texture and properties of commercial copper using chemical etching after applying various extensions and annealing temperatures. For example contamination of the specimens can arise during polishing which cannot be satisfactorily removed by subsequent cleaning and the resulting electron micrographs are of poor quality. Fig. 4a and b show two micrographs of copper samples after ion etching for 3 h in which the annealing temperatures were 400 and 700°C, respectively. The effect of the higher annealing temperature is evident from the much larger size of the crystals in Fig. 4b. Similar observations showed that the crystal size decreases with increasing extension, but the annealing temperature was shown to be the most critical factor.

Fig. 5a shows a micrograph of an ion-etched copper iron sinter, containing 10% copper and 0.2% carbon. Other micrographs taken at lower magnifications showed the grain boundaries and porosity of the material and in Fig. 5a some grains can be seen one of which shows striations characteristic of Pearlite. This is a particular structure of iron containing alternate laminations of ferrite and cementite. Fig. 5b is an X-ray image of Fig. 5a using copper X-rays and clearly shows the distribution of the copper at the grain boundaries. This effect is the inverse of that found with chemical etching when the copper is left behind. It was also noted that the Pearlite structure was not easily observed if the specimen was rotated during etching.

Ion etching glass confirmed the view of Navez *et al.* [19] that the morphology obtained is

essentially a function of the geometry of bombardment and that various types of structure can be obtained depending upon the angle of incidence of the ion beam. Fig. 6 shows a typical structure observed with soda glass in which a system of parallel grooves orientated along the direction of the ion beam can be seen. These are almost certainly artefacts and it would appear that little structural information can be revealed using this technique with glass.

Araldite is an epoxy resin and micrographs shown in Fig. 7a and b taken after ion etching a polished sample for 16 h demonstrate the need for consideration of the thermal effects of ion bombardment. The specimen had been formed against a copper block to act as a thermal sink in an attempt to reduce the temperature of the Araldite. The micrograph in Fig. 7a was taken in a region about 50 μm from the junction and shows a surprisingly regular structure. However, the micrograph in Fig. 7b was taken at a distance of about 1 mm from the junction where the temperature would be higher and shows a very different and

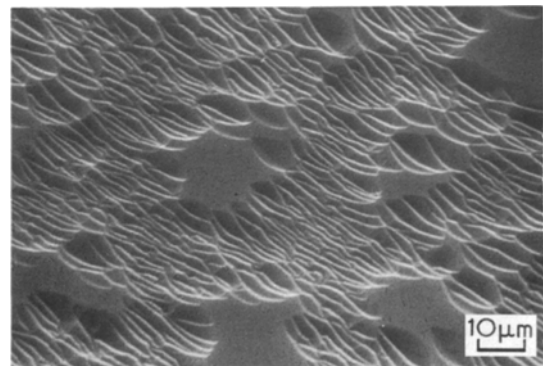


Figure 6 Typical ion etched surface of soda glass.

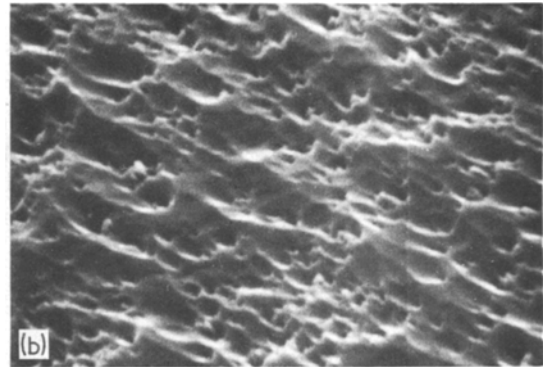
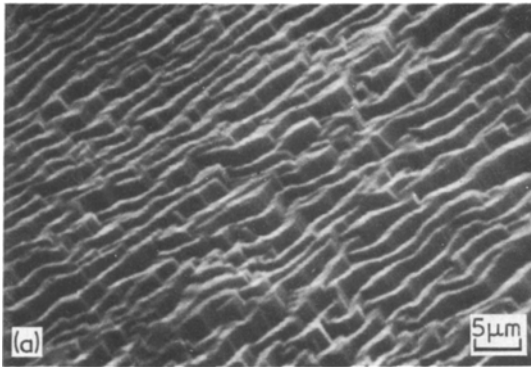


Figure 7 Ion etched surfaces of Araldite; (a) 50 μm and (b) 1 mm from a copper junction.

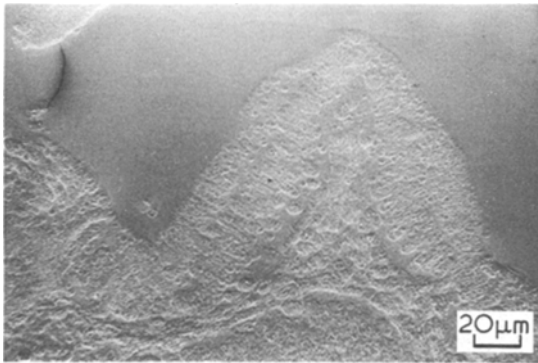


Figure 8 Ion etched surface of a specimen of a rat duodenum.

irregular topography more characteristic of the effects of thermal degradation. At this stage no satisfactory explanation can be given for the apparent regular structure shown in Fig. 7a.

Fig. 8 shows a micrograph after ion etching for 2 h of a specimen of rat duodenum which had been fixed in glutaraldehyde and osmium tetroxide before being embedded in Epon resin. The micro-

graph shows part of the general structure of the villi cells contained within the duodenum and micro-villi cells can also just be seen. It is thought that the observed microstructure is a result of the large variation of the sputtering yield rising from the selective intake of the heavy fixation elements by different parts of the tissue. Thus in contrast to the view of Hodges *et al.* [4], this technique should have useful applications in soft biological tissues.

Various aspects of the structure of the hard biological materials of the human tooth were also studied. Fig. 9a was taken after etching a microtome of a tooth in the region of the amelodentinal junction for 12 h. In the upper part of the micrograph the prismatic structure of the enamel can be seen and the softer dentine in the lower half has clearly been etched much more than the enamel, as shown by the etched step which is about 5 μm in height. Some dentinal tubules extending from the junction into the dentine have also been exposed. These tubules contain nerve fibres and extend into the pulp of the tooth. Fig. 9b shows

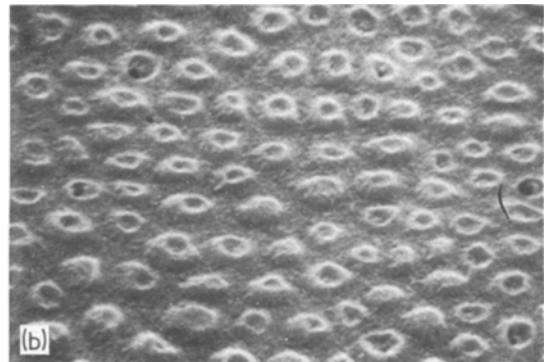
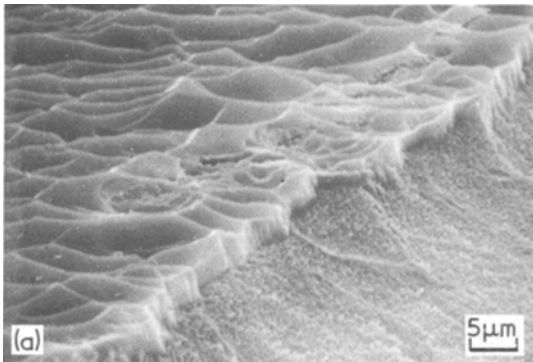


Figure 9 (a) Ion etched surface around the junction between the tooth enamel at the upper and the dentine at the lower half of the micrograph. (b) Ion etched surface of a transverse section of a tooth showing the dentinal tubules.

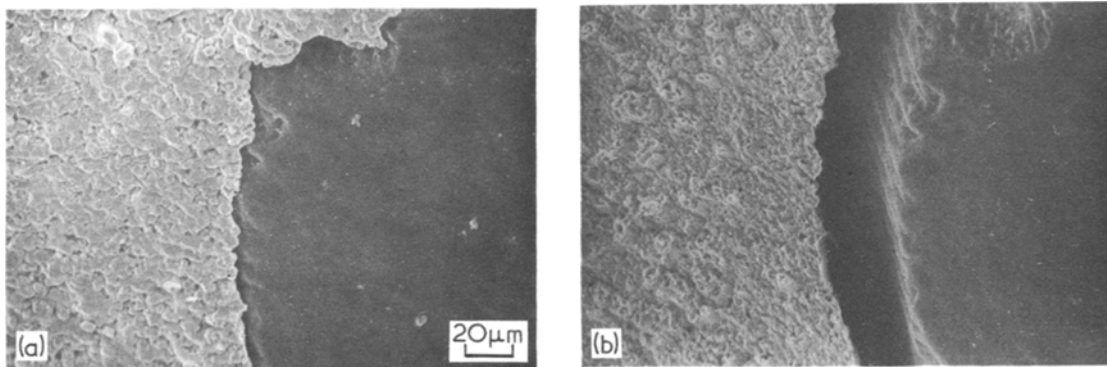


Figure 10 Electron micrographs of a whole tooth showing the amalgam on the left and the enamel on the right, (a) before and (b) after ion etching for 4 h.

an end-on view of the tubules taken from an etched specimen of a transverse section of a tooth.

Other uses of this etching facility have been demonstrated using whole teeth. Fig. 10a shows an electron micrograph of a tooth filled after extraction. A small gap (about $5\ \mu\text{m}$) is clearly visible between the amalgam on the left and the enamel. The micrograph in Fig. 10b was taken of the same area after ion etching for 4 h and the gap has apparently increased to about $30\ \mu\text{m}$. It is thought that this is due to the removal, during etching, of a thin burnished layer about $30\ \mu\text{m}$ thick which has been left after the filling process. Thus it is possible that such a layer could be eroded away in the oral environment to expose the relatively large gap which could allow bacteria to penetrate and possibly produce tooth decay.

5. Conclusions

It has been shown that because of its size and simplicity of construction and operation the saddle field ion source is very suitable for *in situ* ion etching in a SEM. It can be applied to both conducting and insulating materials for in-depth structural studies but can equally well find application in problems when it is required to remove, in a controlled way, thin layers from a sample to reveal the underlying structure.

It is envisaged that it may be possible to modify the arrangement by pulsing the ion and electron beams for simultaneous etching and viewing.

Acknowledgements

The authors would like to acknowledge the support of the Science Research Council for the grant to purchase the scanning electron microscope and one of us (R.S.D.) for an SRC studentship for

one year. The authors would also like to thank the staff at the following establishments for their collaboration at various stages of the work – Oral Pathology Department, University of Birmingham; Physics, Metallurgy and Biology Department, University of Aston in Birmingham; Lucas Research Group, Solihull; Woolfson Institute for Interfacial Technology, Nottingham University and Ciba Geigy, Manchester.

References

1. P. G. GLOERSEN, *J. Vac. Sci. Technol.* **12** (1975) 23.
2. P. NORGATE and V. J. HAMMOND, *Phys. Technol.* **5** (1974) 186.
3. A. D. G. STEWART, Vth International Congress for Electron Microscopy, Philadelphia (1962) D12.
4. G. M. HODGES, M. D. MUIR, C. SELLA and A. J. P. CARTEUD, *J. Microsc.* **95** (1972) 445.
5. M. SPECTOR, S. L. KIMZEY and L. BURNS, Scanning Electron Microscopy, I.I.T.R.I., Chicago, Part III (1974) p. 665.
6. CH. WEISSMANTEL, O. FIELDER, G. REISSE, H. J. ERLER, U. SCHEIT, M. ROST and J. HERBERGER, *Jap. J. Appl. Phys. Suppl. 2, Part 1* (1974) 509.
7. R. SHIMIZU, *Jap. J. Appl. Phys.* **13** (1974) 228.
8. A. H. MCILRAITH, *Nature, London* **212** (1966) 1422.
9. R. K. FITCH, T. MULVEY, W. J. THATCHER and A. H. MCILRAITH, *J. Phys. D.* **3** (1970) 1339.
10. G. J. RUSHTON, K. R. O'SHEA and R. K. FITCH, *ibid* **6** (1973) 1167.
11. J. FRANKS, Brit. Pat. No. 54627, 1972.
12. J. FRANKS and A. M. GHANDER, *Vacuum* **24** (1974) 489.
13. V. A. GUNTHERSCHULZE and W. TOLLMEIN, *Z. F. Phys.* **119** (1942) 685.
14. A. D. G. STEWART and M. W. THOMPSON, *J. Mater. Sci.* **4** (1969) 56.
15. G. K. WEHNER and D. G. HAJICEK, *J. Appl. Phys.* **42** (1971) 1145.

16. D. J. BARBER, F. C. FRANK, M. MOSS, J. W. STEEDS and I. S. T. TSONG, *J. Mater. Sci.* 8 (1973) 1030.
17. I. H. WILSON, *Radiation Effects* 18 (1973) 95.
18. M. J. WITCOMB, *J. Mater. Sci.* 9 (1974) 551.
19. M. NAVEZ, C. SELLA and D. CHAPEROT, "International Symposium on Ionic Bombardment, Theory and Applications" (Gordon and Breach, New York, 1962) p. 339.

Received 9 July and accepted 10 September 1976.